Citation: J. Bermúdez-Cameo, J. P. Barreto, G. López-Nicolás, J. J. Guerrero. Minimal solution for computing pairs of lines in non-central cameras. 12th Asian Conference on Computer Vision (ACCV 2014), Singapore, 1-5 November 2014. Springer International Publishing Switzerland. D. Cremers et al. (Eds.): ACCV 2014, Part I, LNCS 9003, pp. 1-13, 2015

Minimal solution for computing pairs of lines in non-central cameras

Jesus Bermudez-Cameo[1], João P. Barreto[2], Gonzalo Lopez-Nicolas[1] and Jose J. Guerrero[1]

[1]Instituto de Investigación en Ingeniería de Aragón
Universidad de Zaragoza, Spain
bermudez@unizar.es, gonlopez@unizar.es, josechu.guerrero@unizar.es
[2]Institute of Systems and Robotics
University of Coimbra, 3030 Coimbra, Portugal.
jpbar@deec.uc.pt

Abstract. In non-central cameras, the complete geometry of a 3D line is mapped to each corresponding projection, therefore each line can be theoretically recovered from a single view. However, the solution of this problem is ill-conditioned due to the lack of effective baseline between rays. This limitation prevents from a practical implementation of the approach if lines are not close to the visual system. In this paper, we exploit additional geometric constraints to improve the results of line reconstruction from single images in non-central systems. In particular, we obtain the minimal solution for the case of a pair of intersecting orthogonal lines and for the case of a pair of parallel lines considering three rays from each line. The proposal has been evaluated with simulations and tested with real images.

1 Introduction

In any central camera the projection surface of a 3D line is a plane. Any line contained in this plane is projected on the same line-image, and therefore two of the four degrees of freedom (DOF) of the 3D line are lost in the projection. By contrast, in certain non-central cameras (non-central implies that the projecting rays do not intersect in a common point) the projection surface of a line is a ruled surface composed by skew rays (except in certain degenerate cases). Through this surface there exist a unique mapping between a 3D line and its projection on the image (line-image) which can be exploited to recover the geometry of the 3D line from a single image. In particular, four generic rays[1] corresponding to four points on a line projection provide four independent constraints allowing to compute the complete geometry of the 3D line [1]. In practice, this is an ill-posed problem and the geometry of the 3D line can be only recovered if the

[1] Four lines are generic if no two of them are coplanar, no three of them are coconical or cocylindrical, and the four are not cohyperbolic, i.e. do not lie on the same ruled quadric surface.

relative depth of the line with respect to the system dimensions is low enough for guaranteeing effective baseline between rays.

In this paper we exploit the structure of the scene reducing the number of DOFs of the sought solution. In central systems with conventional cameras this idea is used for inferring layouts from line projections which only provide two independent constraints [2, 3] for each line-image. In the case of non-central systems we propose to solve the four DOFs of each line using the redundant independent constraints provided by line projections by imposing geometric constraints between pairs of lines. The proposed geometric constraints are: orthogonal intersection between lines and parallelism between lines reducing to six the number of rays needed for a minimal solution of a pair of lines.

1.1 Previous work

The basis for computing the geometry of the 3D line from a single line projection (line-image) is that given four generic lines there exist only two lines intersecting them [4, 5]. In [1] this reasoning is introduced for application in computer graphics. In [6, 7] this approach is exploited to compute 3D lines from 4 rays in non-central systems comparing the linear approach with different computation methods and considering the degeneracies and singular configurations. In [8] the approach is used with spherical catadioptric mirrors, and in addition two non-central systems are used for reconstruction. Work in [9] extends the approach to planar curves. To improve the accuracy in reconstruction some simplifications have been proposed: considering only horizontal lines [10, 11] or exploiting cross-ratio properties [12]. In [13] the degeneracies caused by the revolution symmetry are avoided using an off-axis system. More recently in [14] the approach is particularized to the case of conical mirrors allowing to compute both the 3D line and the mirror geometry from a single line projection.

1.2 Contributions

In this paper we present the minimal solution for computing a junction composed by two orthogonal intersecting lines and for computing two parallel lines in non-central systems. This allows to obtain the complete geometry of these pairs of lines from three rays belonging to each line in a calibrated non-central system. The interest of this result can be in robust extraction methods based on minimal sets like RANSAC or in the improvement of the reconstruction accuracy in line fitting. The approach has been implemented for spherical catadioptric systems, using the projection model described in [15]. The proposal has been evaluated in simulation, and tested with real images.

2 Recovering a 3D line from four skew generic rays

In this section we present the background, geometric concepts and notation used for computing a 3D line from four generic rays. The description used for lines are the Plücker coordinates based on Grassmann algebra.

2.1 Plücker Coordinates of a Line

The Plücker coordinates of a 3D line is a $\mathbb{P}^5$ representation of a line obtained from the null space of any pair of points $X = \left(x_0, \mathbf{x}^\mathsf{T}\right)^\mathsf{T}$, and $Y = \left(y_0, \mathbf{y}^\mathsf{T}\right)^\mathsf{T}$ belonging to the line. The description of a Plücker line from the coordinates of the defining points are $\mathbf{L} = \left(\mathbf{l}^\mathsf{T}, \overline{\mathbf{l}}^\mathsf{T}\right)^\mathsf{T}$ where $\mathbf{l} \in \mathbb{R}^3$, $\mathbf{l} = x_0\mathbf{y} - y_0\mathbf{x}$ and $\overline{\mathbf{l}} \in \mathbb{R}^3$, $\overline{\mathbf{l}} = \mathbf{x} \times \mathbf{y}$ (depending on the author the order and the sign of the elements can differ, here we follow the standard in [16]).

Notice that not all the elements of the $\mathbb{P}^5$ space correspond to 3D lines. The points of $\mathbb{P}^5$ corresponding to lines in $\mathbb{P}^3$ must hold $\mathbf{l}^\mathsf{T}\overline{\mathbf{l}} = 0$ which is known as Plücker identity. This identity is a quadratic constraint which defines a two dimensional subspace in $\mathbb{P}^5$ called the Klein quadric M_2^4 [16]. Plücker representation has a geometric interpretation in Euclidean geometry. Vector $\mathbf{l}$ represents the direction of $\mathbf{L}$ (see Fig. 1 (a)) and $\overline{\mathbf{l}}$ is the moment vector which can be seen as the normal to a plane passing through the 3D line and the origin of the reference system. The Plücker identity expresses the orthogonality of $\mathbf{l}$ and $\overline{\mathbf{l}}$ given that the direction vector must be contained in the plane defined by $\overline{\mathbf{l}}$. $\mathbf{L}$ is an homogeneous vector but when normalizing respect to $\mathbf{l}$, $\left|\overline{\mathbf{l}}\right|$ is the minimum distance from the origin to the 3D line. Therefore, when normalizing respect to $\overline{\mathbf{l}}$, $|\mathbf{l}|$ is the inverse of that distance.

2.2 Intersection of rays with a 3D line

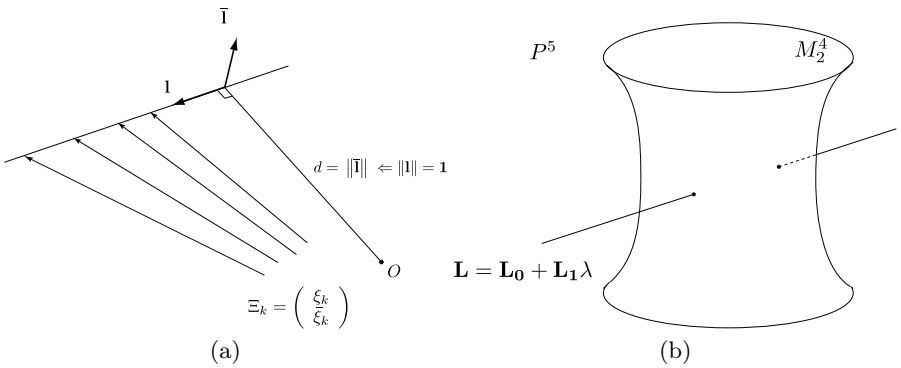

Fig. 1. (a) Plücker description for lines and line projection. (b) One dimensional subspace in $\mathbb{P}^5$ and Klein Quadric.

The constraint resulting of the intersection of a 3D line with a projection ray can be expressed linearly by the side operator which defines the signed distance between two lines $\mathbf{L} = \left(\mathbf{l}^\mathsf{T}, \overline{\mathbf{l}}^\mathsf{T}\right)^\mathsf{T}$ and $\mathbf{M} = \left(\mathbf{m}^\mathsf{T}, \bar{\mathbf{m}}^\mathsf{T}\right)^\mathsf{T}$. It is described as

$$side\,(\mathbf{L}, \mathbf{M}) = \mathbf{L}^\mathsf{T}\mathsf{W}\mathbf{M} = \mathbf{l}^\mathsf{T}\bar{\mathbf{m}} + \overline{\mathbf{l}}^\mathsf{T}\mathbf{m} \tag{1}$$

where $\mathsf{W} = \begin{pmatrix} 0_{3\times3} & I_{3\times3} \\ I_{3\times3} & 0_{3\times3} \end{pmatrix}$.

If the Plücker representation of both skew lines is normalized with the direction vector then this distance is metric in $\mathbb{R}^3$. The sign of this distance depends on the *side* where a line is located with respect to the other (clockwise or counterclockwise). The intersection between two lines is given by the constraint $\mathbf{L}^\mathsf{T}\mathsf{W}\mathbf{M} = 0$. Notice that the self-operation ($side\,(\mathbf{L}, \mathbf{L}) = 0$) becomes the Plücker identity.

A 3D line has four degrees of freedom (DOF), as consequence at least four independent constraints are needed to solve the corresponding equations system. In non-central systems, four projection rays provide four independent constraints when they are generic (Fig 1 (a)). Notice that in a central system the four equations are not independent given that the four rays are coplanar.

However, due to Plücker coordinates set (without taking into account the Plücker identity) is an over-parametrized description of a line, the solution of a system of four homogeneous equations in $\mathbb{P}^5$ is a one dimensional subspace of $\mathbb{P}^5$. The solution of these equations system can be expressed as a singular value decomposition problem in which A is the collection of constraints such that $\mathsf{A}\mathbf{L} = \mathbf{0}$ with $\mathsf{A}_i = \left(\bar{\boldsymbol{\xi}}_i^\mathsf{T}, \boldsymbol{\xi}_i^\mathsf{T}\right)$ where A_i is the i^{th} row of A, in order that it can be written as the product of three matrices, U, Σ,V, such that U and V are orthogonal, Σ is diagonal and $\mathsf{A} = \mathsf{U}\Sigma\mathsf{V}^\mathsf{T}$.

The null space of this system is spanned by the last two columns of V (denoted $\mathbf{L}_0$ and $\mathbf{L}_1$ respectively). The null-space can be parametrized by $\mathbf{L} = \mathbf{L}_0 + \mathbf{L}_1\lambda$ (see Fig. 1 (b)) and imposing the Plücker identity we can compute the intersection of this subspace with the Klein Quadric obtaining two solutions: One is the sought line, the other is the axis of revolution of the visual system if it is axial or an arbitrary line in other case.

Degeneracies There are some cases where the four rays are not independent and the system is degenerated. When the camera is axial the defining rays can be coplanar forming a Planar Viewing Surface (PVS) [7]. These degenerated cases are: the Axial-PVS case when the line is coplanar with the axis of symmetry and the Horizontal-PVS case when all the projecting rays lie in an horizontal plane. If the projection surface of the line is a ruled surface defined by only three rays this surface is called a regulus and the system is also under-determined.

3 Orthogonal junction of two lines

In this section we present the minimal solution for a junction of two orthogonal intersecting lines in non-central systems. Computing a junction composed by two orthogonal intersecting lines is a problem with 6 degrees of freedom (DOF). Four DOFs for one of the 3D lines, other for the depth of the line intersection and the 6th DOF for the angle defining the direction of the orthogonal line.

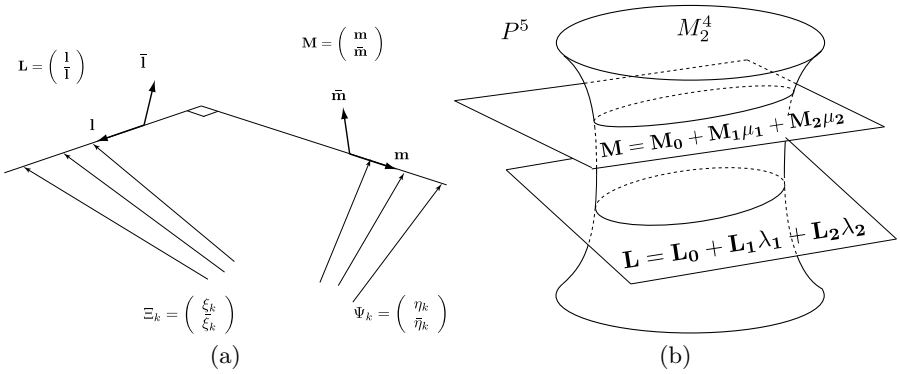

Fig. 2. (a) Orthogonal junction of two lines. (b) Two dimensional subspaces in $\mathbb{P}^5$ and Klein Quadric.

Given the lines $\mathbf{L} = \left(\mathbf{l}^\mathsf{T}, \bar{\mathbf{l}}^\mathsf{T}\right)^\mathsf{T}$, $\mathbf{M} = \left(\mathbf{m}^\mathsf{T}, \bar{\mathbf{m}}^\mathsf{T}\right)^\mathsf{T}$ and considering three generic rays $\boldsymbol{\Xi}_k$ intersecting the line $\mathbf{L}$ and three generic rays $\boldsymbol{\Psi}_k$ intersecting $\mathbf{M}$ (see Fig. 2 (a)), the corresponding null spaces of the under determined linear systems

$$\boldsymbol{\Xi}_k^\mathsf{T} \mathsf{W} \mathbf{L} = 0 \quad , \quad \boldsymbol{\Psi}_k^\mathsf{T} \mathsf{W} \mathbf{M} = 0 \tag{2}$$

are two subspaces of dimension 2 in $\mathbb{P}^5$. These subspaces are not contained in the Klein quadric and intersect the Klein quadric in two one-dimensional curves (see Fig. 2 (b)). A parametrized description of these 2-dimensional subspaces can be obtained by solving the null space of these systems with a singular value decomposition algorithm.

Taking as example the case of $\mathbf{L}$ and $\boldsymbol{\Xi}_k = \left(\boldsymbol{\xi}_k{}^\mathsf{T}, \bar{\boldsymbol{\xi}}_k{}^\mathsf{T}\right)^\mathsf{T}$: the matrix $\mathsf{A} = \begin{bmatrix} \bar{\boldsymbol{\xi}}_1 & \bar{\boldsymbol{\xi}}_2 & \bar{\boldsymbol{\xi}}_3 \\ \boldsymbol{\xi}_1 & \boldsymbol{\xi}_2 & \boldsymbol{\xi}_3 \end{bmatrix}^\mathsf{T}$ can be written as the product of the three matrices, $\mathsf{A} = \mathsf{U}\Sigma\mathsf{V}^\mathsf{T}$ and the null space is spanned by the three last columns of matrix V denoted as $\mathbf{L}_0$, $\mathbf{L}_1$ and $\mathbf{L}_2$ parametrizing it with $L : \mathbb{P}^2 \mapsto \mathbb{P}^5$ defined as

$$\mathbf{L} = \mathbf{L}_0 + \mathbf{L}_1\lambda_1 + \mathbf{L}_2\lambda_2 \sim \mathsf{L}_m \boldsymbol{\lambda} \tag{3}$$

where $\mathsf{L}_m = \begin{bmatrix} \mathbf{L}_0 & \mathbf{L}_1 & \mathbf{L}_2 \end{bmatrix}$ and $\boldsymbol{\lambda} \in \mathbb{P}^2$ with $\boldsymbol{\lambda} = \left(\tilde{\lambda}_0, \tilde{\lambda}_1, \tilde{\lambda}_2\right)^\mathsf{T} \sim (1, \lambda_1, \lambda_2)^\mathsf{T}$.

Analogously, for $\mathbf{M}$ we parametrize the null space with

$$\mathbf{M} = \mathbf{M}_0 + \mathbf{M}_1\lambda_1 + \mathbf{M}_2\lambda_2 \sim \mathsf{M}_m \boldsymbol{\mu} \tag{4}$$

where $\mathsf{M}_m = \begin{bmatrix} \mathbf{M}_0 & \mathbf{M}_1 & \mathbf{M}_2 \end{bmatrix}$ and $\boldsymbol{\mu} \in \mathbb{P}^2$ with $\boldsymbol{\mu} = (\tilde{\mu}_0, \tilde{\mu}_1, \tilde{\mu}_2)^\mathsf{T} \sim (1, \mu_1, \mu_2)^\mathsf{T}$.

To obtain the four parameters λ_1, λ_2, μ_1 and μ_2 we need four additional independent constraints. These constraints are the condition of belonging at the Klein quadric for both lines, the perpendicularity between them and the intersection between them. These constraints are explicitly defined by

$$\mathbf{L}^\mathsf{T}\mathsf{W}\mathbf{L} = 0, \quad \mathbf{M}^\mathsf{T}\mathsf{W}\mathbf{M} = 0, \quad \mathbf{l}^\mathsf{T}\mathbf{m} = 0, \quad \mathbf{L}^\mathsf{T}\mathsf{W}\mathbf{M} = 0 \tag{5}$$

becoming a system of 4 quadratic equations in terms of λ_1, λ_2, μ_1 and μ_2 with the form

$$\boldsymbol{\lambda}^\mathsf{T}\Omega_1\boldsymbol{\lambda} = 0 \quad \text{where} \quad \Omega_1(i,j) = \mathbf{L}_i{}^\mathsf{T}\mathsf{W}\mathbf{L}_j \tag{6}$$

$$\boldsymbol{\mu}^\mathsf{T}\Omega_2\boldsymbol{\mu} = 0 \quad \text{where} \quad \Omega_2(i,j) = \mathbf{M}_i{}^\mathsf{T}\mathsf{W}\mathbf{M}_j \tag{7}$$

$$\boldsymbol{\lambda}^\mathsf{T}\Omega_3\boldsymbol{\mu} = 0 \quad \text{where} \quad \Omega_3(i,j) = \mathbf{l}_i{}^\mathsf{T}\mathbf{m}_j \tag{8}$$

$$\boldsymbol{\lambda}^\mathsf{T}\Omega_4\boldsymbol{\mu} = 0 \quad \text{where} \quad \Omega_4(i,j) = \mathbf{L}_i{}^\mathsf{T}\mathsf{W}\mathbf{M}_j. \tag{9}$$

This system can be manipulated to reduce the number of dimensions but increasing the degree of equations. Given the equations (8) and (9), imagine the $\mathbb{P}^2$ space of $\boldsymbol{\lambda}$ and the lines depending on $\boldsymbol{\mu}$:

$$\mathbf{U} = \Omega_3\boldsymbol{\mu} \quad , \quad \mathbf{V} = \Omega_4\boldsymbol{\mu} \tag{10}$$

Solving these equations for $\boldsymbol{\lambda}$

$$\begin{bmatrix}\mathbf{U}^\mathsf{T}\\ \mathbf{V}^\mathsf{T}\end{bmatrix}\boldsymbol{\lambda} = 0 \tag{11}$$

we obtain an explicit linear morphism

$$\boldsymbol{\lambda} = \mathsf{C}\hat{\boldsymbol{\mu}} \tag{12}$$

where $\hat{\boldsymbol{\mu}} = \left(\tilde{\mu}_0^2, \tilde{\mu}_0\tilde{\mu}_1, \tilde{\mu}_0\tilde{\mu}_2, \tilde{\mu}_1^2, \tilde{\mu}_1\tilde{\mu}_2, \tilde{\mu}_2^2\right)^\mathsf{T} \sim \left(1, \mu_1, \mu_2, \mu_1^2, \mu_1\mu_2, \mu_2^2\right)^\mathsf{T}$.

Substituting $\boldsymbol{\lambda}$ in equation (6) we have a system of two equations with two unknowns, the first is a quartic expression and the second a quadratic equation.

$$\hat{\boldsymbol{\mu}}^\mathsf{T}\mathsf{C}^\mathsf{T}\Omega_1\mathsf{C}\hat{\boldsymbol{\mu}} = 0 \tag{13}$$

$$\boldsymbol{\mu}^\mathsf{T}\Omega_2\boldsymbol{\mu} = 0 \tag{14}$$

Substituting (14) in (13) we obtain a single polynomial equation with one unknown of degree 8 which can be solved for μ_1.

$$\sum_{i=0}^{8} c_i\mu_1^i = 0 \tag{15}$$

From the fundamental theorem of algebra we know that the number of solutions of this polynomial is 8. Using equation (14) we obtain 2 solutions of μ_2 from each solution for μ_1. One solution of (λ_1, λ_2) is obtained from each solution (μ_1, μ_2) (12), therefore the maximum number of solutions is 16. However, the majority of them are removed considering only real solutions , compatible with the equations and coherent with the orientation of the defining rays. Usually only 2 solutions remain.

4 Two parallel lines

In this section we present the minimal solution for computing the geometry of two parallel lines in non-central systems. Computing two parallel lines is a problem with 6 DOFs: in this particular case two DOFs for the common direction and two additional DOFs for each line. From three generic rays $\boldsymbol{\Xi}_k$ intersecting a line $\mathbf{L}$ and three generic rays $\boldsymbol{\Psi}_k$ intersecting a line $\mathbf{M}$ we compute the two dimensional subspaces (see Fig. 2 (b)),

$$\mathbf{L} = \mathbf{L}_0 + \mathbf{L}_1\lambda_1 + \mathbf{L}_2\lambda_2 \sim \mathsf{L}_m\boldsymbol{\lambda} \tag{16}$$

$$\mathbf{M} = \mathbf{M}_0 + \mathbf{M}_1\lambda_1 + \mathbf{M}_2\lambda_2 \sim \mathsf{M}_m\boldsymbol{\mu} \tag{17}$$

To obtain the four parameters λ_1, λ_2, μ_1 and μ_2 we need four additional constraints. First two are the constraint for each line of being in the Klein quadric or being a line,

$$\mathbf{L}^\mathsf{T}\mathsf{W}\mathbf{L} = 0, \tag{18}$$

$$\mathbf{M}^\mathsf{T}\mathsf{W}\mathbf{M} = 0\ . \tag{19}$$

The constraint of being parallels can be expressed as follows,

$$\mathbf{l} = (\mathbf{l}_0 + \mathbf{l}_1\lambda_1 + \mathbf{l}_2\lambda_2) = K\left(\mathbf{m}_0 + \mathbf{m}_1\mu_1 + \mathbf{m}_2\mu_2\right)\ , \tag{20}$$

which means three equations involving an additional unknown K. From (20) it is posible to compute $\boldsymbol{\mu}$ in terms of $\boldsymbol{\lambda}$ obtaining the linear mapping between $\boldsymbol{\mu}$ and $\boldsymbol{\lambda}$

$$\boldsymbol{\mu} = (\mathbf{m}_0, \mathbf{m}_1, \mathbf{m}_2)^{-1}\,(\mathbf{l}_0, \mathbf{l}_1, \mathbf{l}_2)\,\boldsymbol{\lambda}. \tag{21}$$

Substituting $\boldsymbol{\mu}$ in equation (19) we obtain two quadratic equations (18) and (19) depending on $\boldsymbol{\lambda}$,which can be considered as the intersection between two conics in $\mathbb{P}^2$ having four solutions.

5 Simulations

In this section we evaluate the proposed method performing simulations of the line fitting process. As reference method we take the approach of Teller et al. [1] which is denoted as unconstrained linear method.

We consider two different cases: orthogonal junctions and parallel lines. In both cases, a collection of 100 pairs of lines are randomly generated. The length of the lines is 20m. In the case of a junction, the intersection between each pair of lines is located in a cube of side 4 m(see Fig. 3 (a)). In the case of parallel lines, two points are randomly located in a cube of side 4 m and then the orientation on the line is randomly computed (see Fig. 3 (a)). These lines are projected

on an spherical-mirror-based image [15]. The catadioptric system is composed of a spherical mirror with radius of 1.2 m and a perspective camera located at 1.8 m from the center of the sphere. The resolution of the simulated camera is 1024×768.

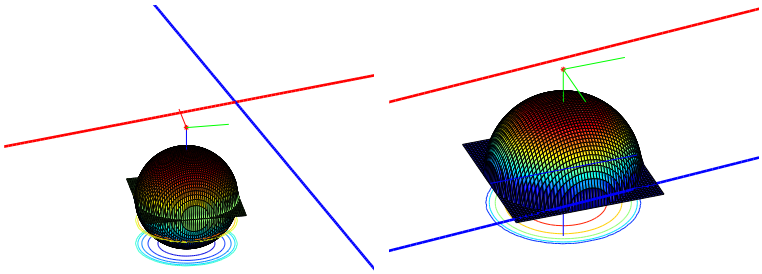

(a) (b)

Fig. 3. Lines configuration example. (a) Junction. (b) Parallel.

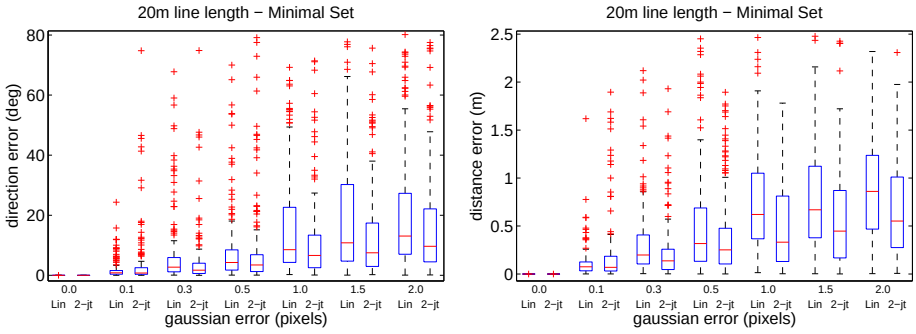

(a) (b)

Fig. 4. Lines estimation using the minimal set of points comparing the linear approach (Lin) and junction approach (2-jt): (a) Direction error (deg) (b) Distance error (m)

Gaussian noise of a given σ is added to the projected points. The value of σ variates from 0.1 to 2. Then 3D lines are computed from its projection in a single image using the linear Teller approach and using our proposal. For each value of σ we compute 100 pairs of lines. The 100 pairs of lines are the same for each value of σ.

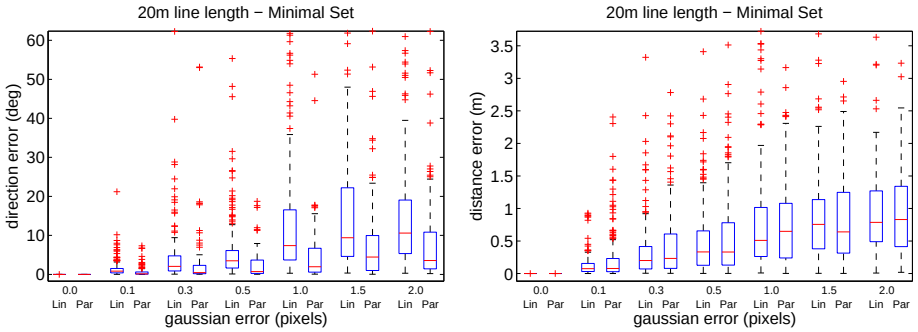

(a) (b)

Fig. 5. Lines estimation using the minimal set of points comparing the linear approach (Lin) and parallel lines approach (Par): (a) Direction error (deg) (b) Distance error (m)

The first simulation, is a comparison between the unconstrained linear approach and our proposals (junction in Fig. 4 and parallel lines in Fig. 5) considering the minimal set of defining points. The length of the lines in this setup is 20m. The linear approach is computed from 8 points (4 for each line) and the proposal (junction or parallel) is computed from 6 points (3 for each line). The 6 points used for the proposal is a subset of the 8 points used for the unconstrained linear approach to avoid biasing. When using orthogonal junctions we take care of not using the intersection between lines which is a degenerated configuration with only 5 independent constraints.

The second simulation, is a comparison between the linear approach and our proposal considering more than the minimal set of points in the fitting. Considering more points (200 points), we obtain a least square fitting of the null spaces of dimension two in $\mathbb{P}^5$ described by L_m and M_m. In this case the number of points is the same for both linear and our proposal.

From the results we conclude that there is an improvement in the accuracy of the extracted lines. As expected, the improvement is more evident in the direction of the extracted line than in depth.

6 Experiments with real images

A reconstruction has been carried out to evaluate the performance of the method using a catadioptric system composed by a spherical mirror seen by a conventional camera with resolution 1280×1024 pixels.

6.1 Calibration of the non-central system

First, the perspective camera has been independently calibrated. As the spherical catadioptric system is always axial the extrinsic parameters to calibrate are

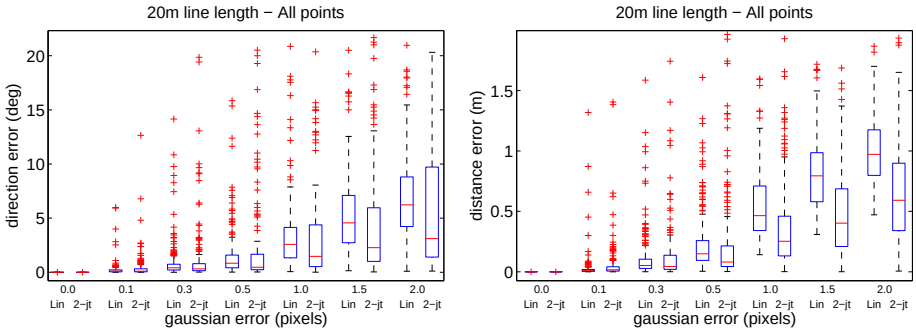

(a) (b)

Fig. 6. Lines estimation using all points comparing the linear approach (Lin) and junction approach (2-jt): (a) Direction error (deg) in 20 m length lines. (b) Distance error (m) in 20 m length lines.

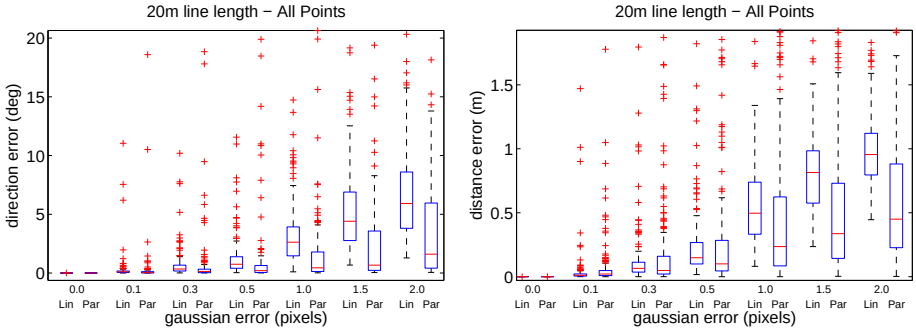

(a) (b)

Fig. 7. Lines estimation of parallel lines using all points comparing the linear approach (Lin) and parallel lines approach (Par): (a) Direction error (deg) in 20 m length lines. (b) Distance error (m) in 20 m length lines.

the tilt in the orientation of the camera, the radius of the sphere r_{sph} and the distance from the center of the sphere to the perspective camera d. Notice that in spherical catadioptric systems d and r_{sph} are coupled in the line projection. Therefore, only $d_{rel} = \frac{d}{r_{sph}}$ can be recovered from a single line-image.

In this case we have computed the tilt in the orientation and the relative distance d_{rel} from the contour projection of the sphere which is a conic in the image plane of the perspective camera and also using the projection of the camera reflection on the image which is related with the direction of the center of the sphere. The radius of the sphere has been estimated from a 3D reconstruction of the mirror obtained from a RGB-D device. This metric can be finally refined using projections of patterns with a known dimension like in the calibration method presented in [17].

6.2 3D line reconstruction

We have performed a reconstruction of four lines forming a rectangle. This disposition allows us to first reconstruct two different junctions and then reconstruct two different sets of parallel lines.

In Fig. 8 we show the forward projection of these four lines after the fitting using the junction. In Fig. 9 we show the reconstructions of these lines from 15 points using the Tellers linear method, our junction approach and our parallel lines approach.

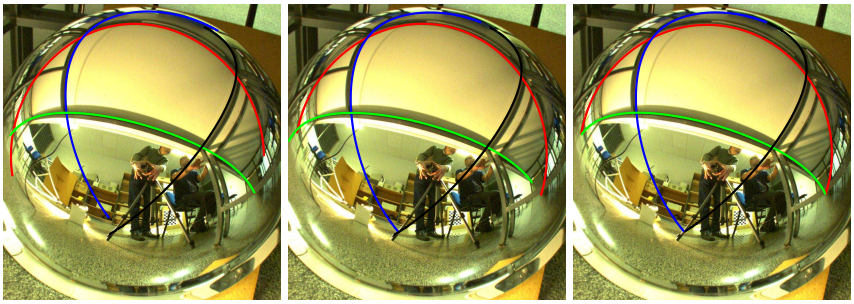

(a) (b) (c)

Fig. 8. Lines projection after fitting: (a) Linear. (b) junction. (c) Parallel.

As we can see in Fig. 8, line projections are very similar in the three cases. However, the reconstructions of the 3D lines are quite different (see Fig. 9). To measure the quality of the results we use the spanned planes by the pairs of lines. In the case of junctions we have compared the planes spanned by the two pairs of intersecting orthogonal lines. Both planes have a deviation of 9.72 degrees. In the case of parallel lines we compare the planes spanned by the two pairs of parallel lines having a deviation of 15.69 degrees. Note that this test is a way to measure quality in orientation but not in depth.

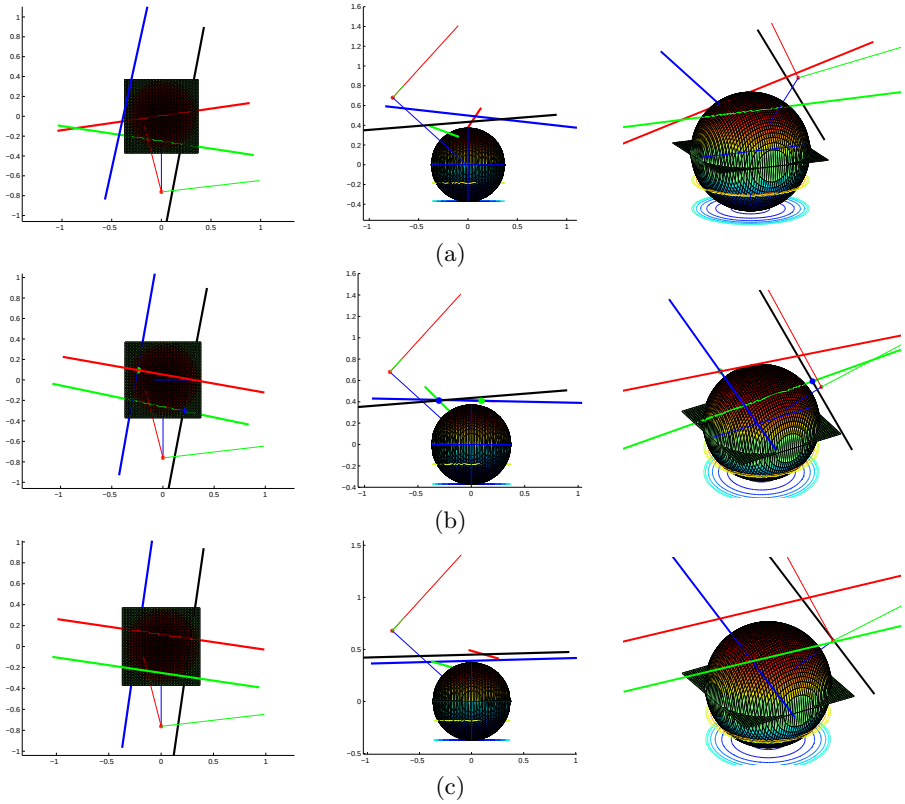

Fig. 9. Reconstructed lines from 15 points, Left XY-View, Middle YZ-View, Right Orthographic-View (a) Teller's method, (b) junction proposal. (c) Parallel proposal

7 Conclusion

In this paper we have presented the minimal solution for computing pairs of intersecting orthogonal lines and parallel lines from single images in non-central systems. This proposal has been tested in the particular case of spherical catadioptric systems. As expected, adding external geometric constraints improve the accuracy of the results. However this improvement does not allow reconstructing lines with lack of effective baseline. Thus, we have not yet solved the impediments for extensively using this kind of systems. The relation between the dimensions of the scene to reconstruct and the dimensions of the system is still too low in practice. Future work inevitably passes through designing new kind of catadioptric or dioptric systems with a bigger effective baseline by construction. Additionally, notice that all the techniques proposed in this paper could be directly used in combination with these systems.

Acknowledgement. This work was supported by the Spanish project VINEA DPI2012-31781 and FEDER funds. First author was supported by the FPU program AP2010-3849.

References

1. Teller, S., Hohmeyer, M.: Determining the lines through four lines. Journal of graphics tools **4** (1999) 11–22
2. Lee, D.C., Hebert, M., Kanade, T.: Geometric reasoning for single image structure recovery. In: IEEE Conference on Computer Vision and Pattern Recognition (CVPR 2009), 2136–2143
3. Ramalingam, S., Brand, M.: Lifting 3D manhattan lines from a single image. In: IEEE International Conference on Computer Vision (ICCV 2013), 497–504
4. Semple, J. G., Kneebone, G. T.: Algebraic projective geometry. Oxford University Press, USA (1998)
5. Griffiths, P., Harris, J.: Principles of algebraic geometry. Volume 52. John Wiley & Sons (2011)
6. Caglioti, V., Gasparini, S.: On the localization of straight lines in 3D space from single 2D images. In: IEEE Computer Society Conference on Computer Vision and Pattern Recognition (CVPR 2005). Vol. 1 1129–1134
7. Gasparini, S., Caglioti, V.: Line localization from single catadioptric images. International journal of computer vision **94** (2011) 361–374
8. Lanman, D., Wachs, M., Taubin, G., Cukierman, F.: Reconstructing a 3D line from a single catadioptric image. In: Third International Symposium on 3D Data Processing, Visualization, and Transmission (3DPVT 2006), 89–96
9. Swaminathan, R., Wu, A., Dong, H., et al.: Depth from distortions. In: The 8th Workshop on Omnidirectional Vision, Camera Networks and Non-classical Cameras (OMNIVIS 2008)
10. Pinciroli, C., Bonarini, A., Matteucci, M.: Robust detection of 3D scene horizontal and vertical lines in conical catadioptric sensors. In: The 6th Workshop on Omnidirectional Vision (OMNIVIS 2005)
11. Chen, W., Cheng, I., Xiong, Z., Basu, A., Zhang, M.: A 2-point algorithm for 3D reconstruction of horizontal lines from a single omni-directional image. Pattern Recognition Letters **32** (2011) 524–531

12. Perdigoto, L., Araujo, H.: Reconstruction of 3D lines from a single axial catadioptric image using cross-ratio. In: 21th International Conference on Pattern Recognition (ICPR 2012), 857–860
13. Caglioti, V., Taddei, P., Boracchi, G., Gasparini, S., Giusti, A.: Single-image calibration of off-axis catadioptric cameras using lines. In: International Conference on Computer Vision (ICCV 2007), 1–6
14. Bermudez-Cameo, J., Lopez-Nicolas, G., Guerrero, J.J.: Line-images in cone mirror catadioptric systems. In: 22nd International Conference on Pattern Recognition (ICPR 2014)
15. Agrawal, A., Taguchi, Y., Ramalingam, S.: Analytical forward projection for axial non-central dioptric and catadioptric cameras. In: European Conference on Computer Vision (ECCV 2010), 129–143
16. Pottmann, H., Wallner, J.: Computational line geometry. Springer (2001)
17. Agrawal, A., Ramalingam, S.: Single image calibration of multi-axial imaging systems. In: IEEE Computer Society Conference on Computer Vision and Pattern Recognition (CVPR 2013), 1399–1406